Light absorption distribution of uterine tissue filled with strong scattering medium irradiated by diffused light source*

LIN Yong-ping (林永平)[1,2]**, **LIU Lan-tian** (刘蓝天)[2], **LI Zhi-fang** (李志芳)[2], **CAI Jian-yong** (蔡坚勇)[2], and **LI Hui** (李晖)[2]

1. School of Optoelectronic and Communication Engineering, Xiamen University of Technology, Xiamen 361024, China

2. College of Photonic and Electronic Engineering, Fujian Normal University, Fuzhou 350007, China

(Received 16 January 2018 ; Revised 7 May 2018)

Determining the light absorption distribution (LAD) of uterine tissue helps the detection of endometrial carcinoma. In this work, a 3-dimensional optical model of the human uterus is proposed and examined. The model is filled with strong scattering medium (undiluted raw and homogenized milk, URHM) or air at 630 nm and 800 nm wavelengths. Monte Carlo simulations are used to find the absorption profiles of photons by transcervical laser illumination, with a cylindrically diffused light source (CDLS) or spherically diffused light source (SDLS). The results show that 800 nm is a good laser wavelength value for the detection of endometrial carcinoma by photoacoustic imaging (PAI). At the same time, the shape of the light source becomes less important in a relatively large cavity. The impacts of different scattering coefficients of CDLS on the irradiated area are demonstrated. Strong scattering medium is helpful to the illumination of the uterus cavity.

Document code: A **Article ID:** 1673-1905(2018)05-0396-5

DOI https://doi.org/10.1007/s11801-018-8011-3

Cancer of the uterus is also called uterine cancer, womb cancer, cancer of the lining of the womb or endometrial cancer. The most common symptom of cancer of the uterus is unusual vaginal bleeding, particularly any bleeding after menopause[1]. In the western world, endometrial carcinoma is the most common female genital tract malignancy, accounting for nearly 50% of all new gynecologic cancers. Worldwide, it is only the second to cervical cancer in frequency among female genital tract cancers[2–4]. In China, cancers of the uterine corpus are the fifth most common for women and have a significantly upward trend in age-standardized incidence rates[5].

Technology capable of reliably diagnosing endometrial carcinoma in earlier stages or before the development of invasive disease could reduce the mortality and the large economic impact of this disease. Photoacoustic imaging (PAI) is a promising technique that is non-ionizing, low-cost, and offers high-contrast imaging of both the surgical tools and photoabsorbers that are often encountered in diagnostic and therapeutic techniques[6,7]. In PAI, the tissue is irradiated usually by a short-pulsed laser beam to achieve a thermal and acoustic impulse response. Locally absorbed light is converted into heat, which is further converted to a pressure rise via thermoelastic expansion. The initial pressure rise propagates as an ultrasonic wave, which is referred as a photoacoustic wave[8]. Absorption by water is minimal in the near-infrared region (NIR) of the spectra, and absorption by blood is large[9]. The abnormal growth of cancerous cells requires elevated supply of blood vessel network and oxygen than normal tissue, which triggers rapid growth of complex blood vessel networks or tumor angiogenesis[10]. Thus, PAI could be a potential tool to image tumor angiogenesis development and detect endometrial carcinoma in earlier stages. The distribution characteristic of absorbed light energy would determine the imaging depth and range of PA imaging.

Photodynamic therapy (PDT) is a method of tumor treatment employing photosensitizers and laser light for abnormalities of the uterus. Meanwhile, interstitial laser photocoagulation (ILP) is a solution for the thermal ablation of fibroids. The smallest penetration depth occurs for light at 630 nm in myometrium, which has a value less than 2.4 mm. This shallow depth may be desirable for PDT treatments where the clinician wants to minimize

* This work has been supported by the National Natural Science Foundation of China (Nos.61675043 and 81571726), the Young and Middle-aged Teachers Education Research Project of Fujian Province (Nos.JA15383 and JA15375), and the Fujian Provincial Key Laboratory of Optoelectronic Technology and Devices.

** E-mail: pr162@163.com

the necrosis to the outer layers of the uterus associated with endometrial ablation. PDT for ablation of the uterine endometrium is the most unlikely to affect any tissue beyond the myometrium, and the region around 800 nm is the most effective for ablation of fibroids using ILP as the penetration depth of light[11]. The two wavelengths of 630 nm and 800 nm were both considered to get the light propagation of the uterus. Undiluted raw and homogenized milk (URHM) was filled into the cavity of the uterus. The light distribution might be more homogenous in the cavity of the uterus.

In the previous work of our team, the light absorption distribution (LAD) of prostate tissue irradiated by diffused light source was discussed[12]. A photoacoustic method combined with Monte Carlo simulation was used to estimate the 3-D light distribution produced by a cylindrical diffuser which interposed into tissues[13]. In this paper, in order to gain a deeper understanding of light absorption and optimize light delivery in PAI, Monte Carlo simulation for light transport in tissues has been carried out with two diffused light sources. Moreover, the LAD of the whole model filled with air and the URHM excited by the laser with 630 nm and 800 nm wavelengths were also studied.

The human uterus is upside-down pear-shaped and about 7.6 cm in length, 4.5 cm in width (side to side) and 3.0 cm in thickness[14]. It sits low in the abdomen between the bladder and rectum, and is held there by muscle. It is joined to the vagina by the cervix, which is the neck of the uterus. The uterus has three layers, which together form the uterine wall. From innermost to outermost, these layers are endometrium, myometrium and perimetrium[15]. The myometrium is the main part of the uterine wall so that endometrium and perimetrium are neglected. The histological structure of the uterus is shown in Fig.1(a). A 3D triangular mesh optical model of the uterus was built by the histological structure through MATLAB as shown in Fig.1(b) with a size of 50 mm×50 mm×76 mm. The triangular meshes are expressed as off file. Off file uses the surface of object to represent the geometry of the object, and then the surface of the object is divided into a large number of triangles.

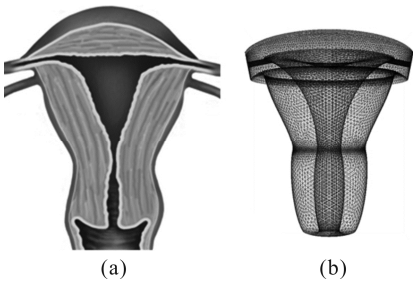

Fig.1 (a) Histological structure and (b) 3D optical model of uterus

Monte Carlo simulations were implemented based on the latest published Monte Carlo software named Molecular Optical Simulation Environment (MOSE 2.3)[16]. It is a powerful tool to solve the forward problems in diffuse optical tomography, fluorescence molecular tomography, and bioluminescence tomography.

To investigate the light propagation beyond the uterus in an optically scattering medium, a 3-D Monte Carlo simulation was performed with a 66 mm×66 mm×84 mm homogeneous background tissue and a resolution cell of 0.1 mm in each dimension as shown in Fig.2.

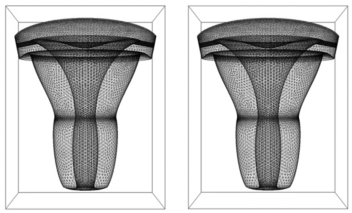

Fig.2 3D mesh optical models of the uterus by (a) SDLS and (b) CDLS

Normally, three different shapes of the light source (cylinder, sphere, and cube) will be considered in the light propagation simulation. The isotropic cubically diffused light source and spherically diffused light source (SDLS) will have almost the same effect due to their size is small compared with the uterus. Under this consideration, the isotropic cubically diffused light won't be studied. An isotropic cylindrically diffused light source (CDLS) with a height of 2 cm and radius of 0.3 mm and an isotropic SDLS with a diameter of 0.6 mm are set in the middle of the cavity of the uterus (z=−10 mm). The azimuth angles of the two diffused light sources were from 0º to 360º and deflection angles were from 0º to 180º to simulate the diffused light. The two continuous wave (CW) lasers wavelengths were set to 630 nm and 800 nm, respectively. The total energy of incident light was 1 J. The recording range of light distribution in this simulation was always kept as x-axis (−33,33) mm, y-axis (−33,33) mm, z-axis (−32,52) mm since the center position of the model was at (0 mm, 0 mm, −10 mm), and the recording steps were set to 0.3 mm. The total incident photon number was 500 000 and the energy of incident light was set as 1. Cartesian coordinates were used for the simulation.

According to optical properties of ex vivo human uterus[11] and Vis/NIR bulk optical properties of milk[17,18], main optical properties, i.e. absorption coefficient μ_a, scattering coefficient μ_s, anisotropy factor g, and refractive index n at 630 nm and 800 nm wavelengths for optical model of uterus and surrounding tissue were specified as Tab.1. Absorption coefficient differs due to differences in water and hemoglobin content. For example, post-menopausal uterus absorption may have been a consequence of its small size, reduced water content and relatively high blood volume. In contrast, the low fibroid absorption is consistent with its poor vascularity[17].

Tab.1 Optical parameters of the simulation model

Tissue	μ_a (mm^{-1})	μ_s (mm^{-1})	g	n
Cavity of uterus	10^{-5}	10^{-5}	1	1
URHM 630 nm	0.014	52	0.95	1.34
URHM 800 nm	0.014	50	0.96	1.34
Myometrium 630 nm	0.044	13	0.9	1.4
Myometrium 800 nm	0.011	9.1	0.9	1.4

In order to analyze the impact of the scattering coefficient on the LAD in the uterine cavity, MC simulations were also implemented by CDLS and SDLS filled with different scattering coefficient (from 10^{-4} mm^{-1} to 10^{2} mm^{-1}) materials at wavelength of 800 nm.

LAD simulation results of two irradiation light sources filled with air or URHM at 630 nm and 800 nm in *yz*-plane are shown in Fig.3. Fig.3(a), (c), (e) and (f) were excited by two different diffused light sources filled with air at wavelength of 630 nm. Meanwhile, Fig.3(b), (d), (f) and (h) were excited by two different diffused light sources at wavelength of 800 nm. The relative light absorption values in Fig.3(a), (c), (e) and (g) are larger than those in Fig.3(b), (d), (f) and (h) due to the small optical absorption coefficient of myometrium at 630 nm.

Comparing Fig.3(a) and Fig.3(c), Fig.3(b) and Fig.3(d), slight differences were obtained by the absorption distribution of uterus excited by the CDLS and SDLS filled with air. However, the differences are hard to identify by eyes. It is also difficult to distinguish the differences of the LAD of uterus produced by the CDLS and SDLS filled with URHM in Fig.3(e) and Fig.3(g), Fig.3(f) and Fig.3(h). But the profiles of LAD of the two laser sources can be easily observed. The shapes of LAD of CDLS are oval while those of SDLS look like circle.

By looking into Fig.3(a) to (d) and Fig.3(e) to (h), large differences will be obtained by the LAD of the model filled with air and URHM. The whole model filled with URHM absorbs the light energy and shows the LAD of the whole model. On the contrary, the whole model filled with air doesn't absorb the light energy and shows an empty cavity in the LAD of the whole model. The relative light absorption values in Fig.3(a) and (b) are smaller than those in Fig.3(e) and (f). It indicates that LAD of the model filled by URHM will be more homogenous. Such a phenomenon also happens in Fig.3(c), (d) and Fig.3(g), (h).

LADs of uterine model produced by CDLS filled with URHM at 800 nm in *yz*-plane and *xz*-plane are shown in Fig.4(a) and (b), respectively. The same LADs of uterine model were found in two planes except the fallopian tube which can only be observed in *yz*-plane. Since the 3-D uterine model was designed in cylindrical symmetry along *z*-axis except the fallopian tube, we have enough reason to believe that the same would be true for the model produced by CDLS or SDLS filled with air or URHM at wavelengths of 630 nm or 800 nm.

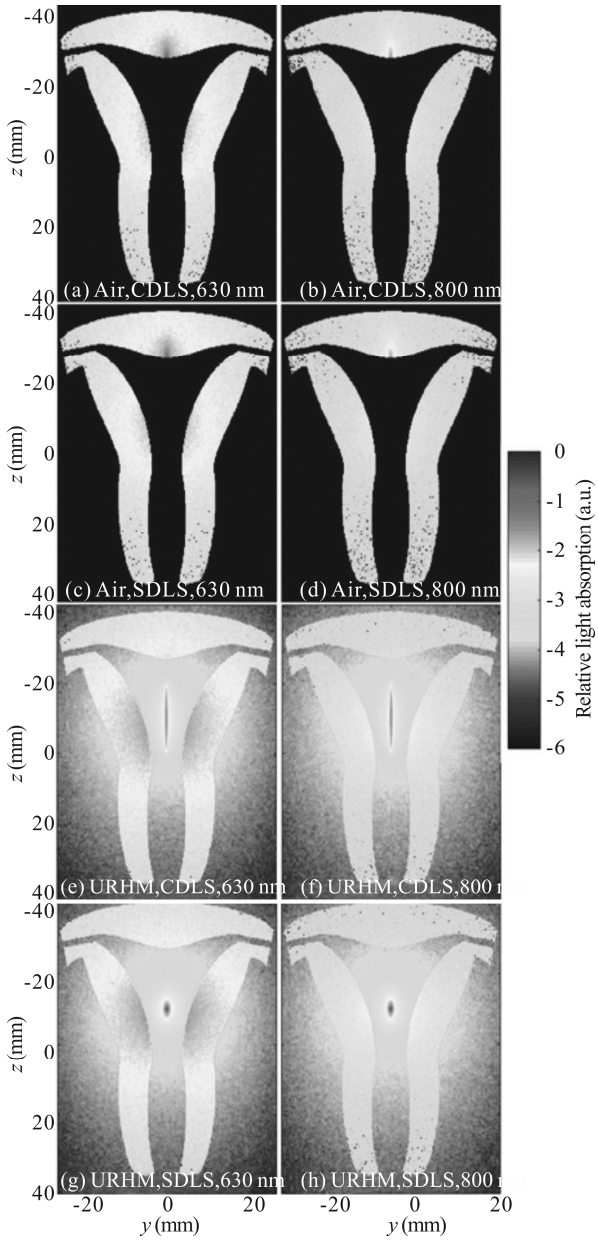

Fig.3 LAD of uterine model in *yz*-plane

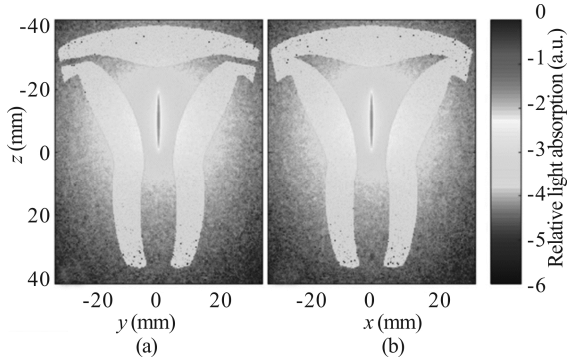

Fig.4 LAD of uterine model produced by CDL filled with URHM at wavelength of 800 nm in (a) *yz*-plane and (b) *xz*-plane, respectively

In order to give a quantitative comparison of irradiated

range by the two diffused light sources filled with air and water at wavelengths of 630 nm and 800 nm, absorbed light energy distribution profiles through the center of the light source (z=−10 mm) along the y-axis were analyzed.

To begin with, profiles of LAD of uterine model at wavelengths of 630 nm and 800 nm through the center of the light source are shown in Fig.5. The relative light absorption values of the uterus at wavelength of 630 nm are significantly higher than those at wavelength of 800 nm by the two different light sources filled with air or URHM. The light absorption of uterine wall is supposed to be smaller as possible so that the tumor can absorb more light energy for easy detection. Under this consideration, 800 nm will be a better choice for PAI than 630 nm.

In addition, profiles of LAD of uterine model produced by CDLS and SDLS through the center of the light source are shown in Fig.6. Different shapes of light sources do not seem to make a difference for the LAD of uterus although a difference can be obtained in the center of the light source. This could be rational because the light sources are not very close to the uterine wall. We can figure out the values of relative light absorption by the two different diffused light sources fall down to the same level very quickly. That is why the light absorption distributions of the uterus are similar so that the shapes of the light sources have the same effect. In other words, the shape of the light source is less important when the fiber is put in the center of a relatively large cavity. In the real world, the cavity of the uterus will be very complicated for women. The upper uterine wall sticks to the lower uterine wall sometimes in pre-menopause or post-menopause women. Under this consideration, we will use the CDLS which can affect bigger area when it is close to the uterine wall in the future.

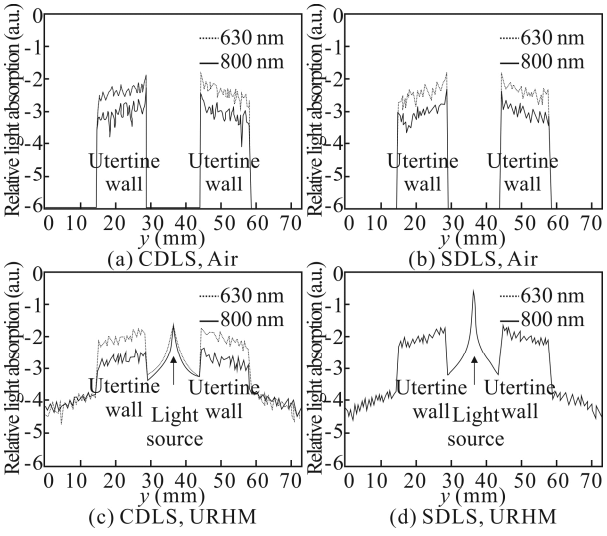

Fig.5 Profiles of LAD of uterine model at wavelengths of 630 nm and 800 nm through the center of the light source (z=-10 mm)

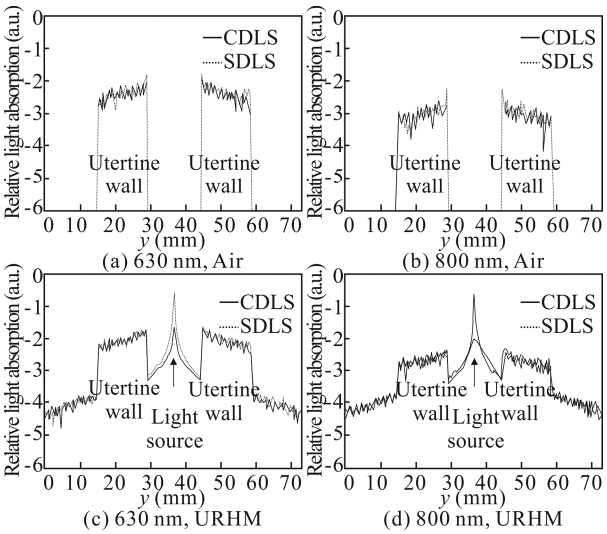

Fig.6 Profiles of LAD of uterine model produced by CDLS and SDLS through the center of the light source (z=-10 mm)

Last but not least, profiles of LAD of uterine model filled with air or URHM through the center of the light source are shown in Fig.7. The relative light absorption values of uterus filled with URHM are higher than those of uterus filled with air. That is to say, the URHM facilitates the light propagation. This also indicates that a material which has an extremely small absorption coefficient and an extremely big scattering coefficient is helpful to the light delivery in the uterus cavity.

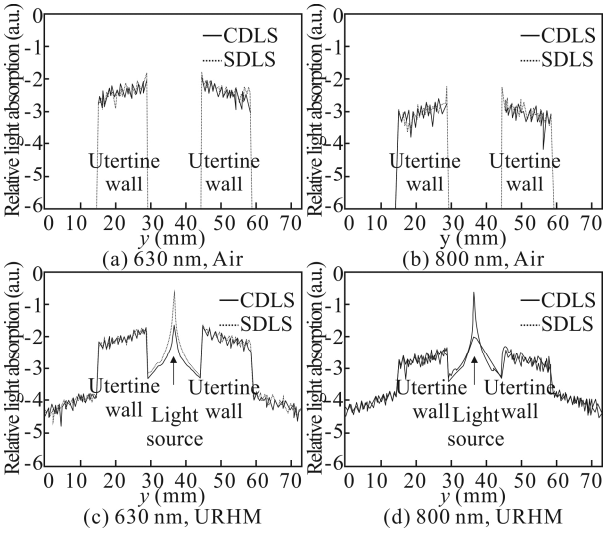

Fig.7 Profiles of LAD of uterine model filled with air or URHM through the center of the light source (z=-10 mm)

The results of the irradiated area in yz-plane (x=0 mm) produced by CDLS and SDLS respect to scattering coefficients from 10^{-4} mm^{-1} to 10^{2} mm^{-1} are shown in Fig.8(a).

It can be seen that there is a peak value in each of line. Moreover, the irradiated area of CDLS is larger than the area of SDLS. The peak values of CDLS and SDLS are found at the scattering coefficients of 5 mm^{-1} and 6 mm^{-1}, respectively. As we know, higher scattering coefficient facilitates the light delivery in the tissue. However, higher scattering coefficient increases the chance of absorption. Thus, a relative irradiated area is defined as irradiated area times μ_s/μ_a. The results of the relative irradiated area are shown in Fig.8(b). A significant increase was found in the relative irradiated area as the increase of scattering coefficient. The ratio of scattering coefficient and absorption coefficient has a considerable impact on the irradiated area. That is to say, the material which has an extremely small absorption coefficient and an extremely big scattering coefficient helps the light delivery in uterus cavity.

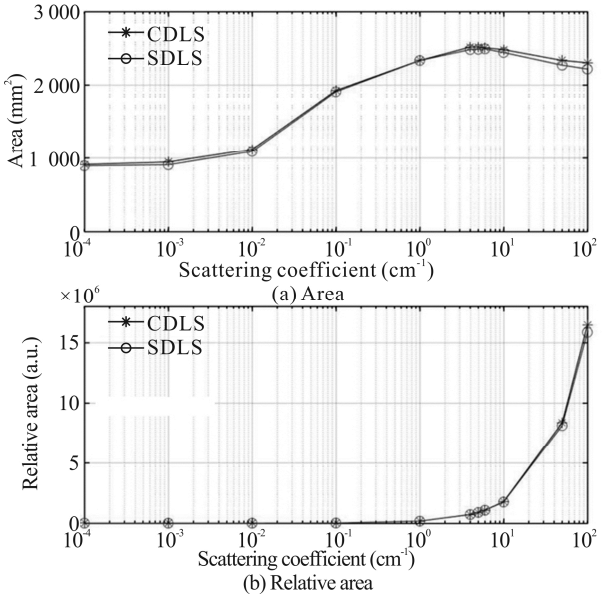

Fig.8 Results of the irradiated area in *yz*-plane (*x*=0 mm) produced by CDLS and SDLS respect to scattering coefficients from 10^{-4} mm^{-1} to 10^{2} mm^{-1}

In this paper, light propagation and absorption were successfully simulated by using the designed 3D model of uterus filled with air or URHM employing Monte Carlo simulation by two different diffused light sources at 630 nm and 800 nm wavelengths. The simulation results show that the laser with a wavelength of 800 nm is good for detection of endometrial carcinoma by PAI. On the contrary, the shapes of light sources are not important since the fiber of the light source has a distance from the uterine wall. Material like URHM which has an extremely small absorption coefficient and an extremely big scattering coefficient is helpful to the illumination of the uterus cavity.

References

[1] Cancer Council, Understanding Cancer of the Uterus, Cancer Council Australia, 2017.

[2] Arora V and Quinn M A, Best Practice & Research Clinical Obstetrics & Gynaecology **26**, 311 (2012).

[3] American Cancer Society, Cancer Facts & Figures 2017, American Cancer Society, 2017.

[4] Torre L A, Bray F, Siegel R L, Ferlay J, Lortet-Tieulent J and Jemal A, CA: A Cancer Journal for Clinicians **65**, 87 (2015).

[5] Chen W, Zheng R, Baade P D, Zhang S, Zeng H, Bray F, Jemal A, Yu X Q and He J, CA: A Cancer Journal for Clinicians **66**, 115 (2016).

[6] Taruttis A and Ntziachristos V, Nature Photonics **9**, 219 (2015).

[7] Zhou Y, Liang J and Wang L V, Journal of Biophotonics **9**, 208 (2016).

[8] Wang L V, IEEE Journal on Selected Topics in Quantum Electronics **14**, 171 (2008).

[9] Manohar S and Razansky D, Advances in Optics and Photonics **8**, 586 (2016).

[10] Kumavor P D, Alqasemi U, Tavakoli B, Li H, Yang Y, Sun X, Warych E and Zhu Q, Journal of Biophotonics **6**, 475 (2013).

[11] Ripley P M, Laufer J G, Gordon A D, Connell R J and Bown S G, Physics in Medicine & Biology **44**, 2451 (1999).

[12] Peng D and Li H, Laser & Optoelectronics Progress **52**, 121703 (2015).

[13] Wenming Xie, Yubin Liu, Zhifang Li and Hui Li, Chinese Optics Letters **12**, 51702 (2014).

[14] Daftrey S and Chakravarti S, Manual of Obstetrics, 2014.

[15] Getz G, Gabriel S B and Cibulskis K, Nature **497**, 67 (2013).

[16] Ren S, Chen X, Wang H, Qu X, Wang G, Liang J and Tian J, ed C M AegerterPLoS ONE **8**, e61304 (2013).

[17] Aernouts B, Van Beers R, Watté R, Huybrechts T, Lammertyn J and Saeys W, Journal of Dairy Science **98**, 6727 (2015).

[18] Aernouts B, Van Beers R, Watté R, Huybrechts T, Jordens J, Vermeulen D, Van Gerven T, Lammertyn J and Saeys W, Colloids and Surfaces B: Biointerfaces **126**, 510 (2015).